JCMM
Available online at
www.jcmm.ro
www.jcmm.org

J. Cell. Mol. Med. Vol 10, No 4, 2006 pp. 922-932

Liver fibrogenesis due to cholestasis is associated with increased Smad7 expression and Smad3 signaling

H. Seyhan [a, #], J. Hamzavi [b, #], Eliza Wiercinska [b], A. M. Gressner [c], P. R. Mertens [d], J. Kopp [a], R. E. Horch [a], Katja Breitkopf [b], S. Dooley [b, *]

[a] Department of Plastic and Hand Surgery, University Medical Center Erlangen, Germany,
[b] Center of Molecular Alcohol Research, II. Medical Clinic, Faculty of Medicine Mannheim, University of Heidelberg, Germany
[c] Institute of Clinical Chemistry and Pathobiochemistry, RWTH University Hospital Aachen, Germany,
[d] Department of Clinical Immunology and Nephrology, RWTH University Hospital Aachen, Germany

Received: June 20, 2006; Accepted: October 30, 2006

Abstract

Background/Aims: Profibrogenic TGF-β signaling in hepatic stellate cells is modulated during transdifferentiation. Strategies to abrogate TGF-β effects provide promising antifibrotic results, however, *in vivo* data regarding Smad activation during fibrogenesis are scarce. **Methods**: Here, liver fibrosis was assessed subsequent to bile duct ligation by determining liver enzymes in serum and collagen deposition in liver tissue. Activated hepatic stellate cells were identified by immunohistochemistry and immunoblots for alpha smooth muscle actin. Cellular localization of Smad3 and Smad7 proteins was demonstrated by immunohistochemistry. RTPCR for Smad4 and Smad7 was conducted with total RNA and Northern blot analysis for Smad7 with mRNA. Whole liver lysates were prepared to detect Smad2/3/4 and phospho- Smad2/3 by Western blotting. **Results**: Cholestasis induces TGF-β signaling *via* Smad3 *in vivo*, whereas Smad2 phosphorylation was only marginally increased. Smad4 expression levels were unchanged. Smad7 expression was continuously increasing with duration of cholestasis. Hepatocytes of fibrotic lesions exhibited nuclear staining Smad3. In contrast to this, Smad7 expression was localized to activated hepatic stellate cells. **Conclusions**: Hepatocytes of damaged liver tissue display increased TGF-β signaling *via* Smad3. Further, negative feedback regulation of TGF-β signaling by increased Smad7 expression in activated hepatic stellate cells occurs, however does not interfere with fibrogenesis.

Keywords: TGF-β • signal transduction • Smad • hepatic stellate cells • hepatocytes • liver fibrogenesis

Introduction

Fibrosis is a characteristic of chronic liver disease irrespective of the underlying etiology. Hepatic stellate cells (HSCs) trigger pathogenesis due to liver damage dependent activation [1]. Activated HSCs transdifferentiate to myofibroblasts (MFBs) that exhibit a synthesis profile predisposing to increased extracellular matrix (ECM) deposition. These encompass proliferation induced by expression of mitogenic cytokines and their receptors; morphologic changes with loss of vitamin A droplets; con-

* Correspondence to: Steven DOOLEY
Department of Medicine II, Gastroenterology and Hepatology, University Hospital, Theodor-Kutzer Ufer 1-3, 68135 Mannheim, Germany.
Tel.: 0049-621-383-3768
E-mail: Steven.dooley@med.ma.uni- heidelberg.de

doi:10.2755/jcmm010.004.14

tractility provided by α smooth muscle actin (SMA) fiber formation leading to constriction of sinusoidal blood flow; and increased synthesis and release of fibrillar collagens [2]. Therapeutic approaches aim to suppress activation of HSCs. One promising route is to antagonize profibrogenic signaling of transforming growth factor β (TGF-β) [3, 4]. TGF-β family members control cellular processes, including proliferation, differentiation and migration. They signal through heteromeric complexes consisting of type I and type II transmembrane receptor serine kinases [5]. Upon activation, type I receptors associate with and activate Smad2 and/or Smad3, two mediators of the Smad protein family. Activated Smad2 and/or Smad3 associate with the common mediator Smad4 and translocate to the nucleus, where Smad protein complexes participate in transcriptional activation of target genes. The TGF-β/Smad signaling cascade contains an autoinhibitory feedback loop involving Smad7 [6, 7]. Smad7 interacts with ligand-activated type I receptors and interferes with receptor binding and phosphorylation of substrate Smads [8]. The Smad7 gene is highly regulated, *e.g.* following incubation with a variety of cytokines like TNF-α, IFN-γ, EGF and TGF-β itself [9–12]. Paracrine and autocrine stimulation of HSCs by TGF-β is a prerequisite for HSC activation and ECM deposition in damaged liver. TGF-β signaling is modulated during transdifferentiation of primary cultured cells [13]. Quiescent HSCs (2 days in culture) are sensitive to exogenous TGF-β, display Smad2/3 phosphorylation, binding to and activation of a Smad binding element (SBE) containing genes and transiently induce Smad7 expression [14]. In contrast activated HSCs (7 days in culture) are not equally responsive to TGF-β [15]. Furthermore, increased expression of TGF-β and constitutively phosphorylated Smad3 in activated HSCs indicate autocrine stimulation [16–19]. Since TGF-β also induces Smad7 expression in quiescent HSCs, a tightly controlled TGF-β signaling is anticipated, whereas lack of Smad7 expression in autocrine activated MFBs could be relevant for the pathogenesis of progressive liver fibrosis. This assumption is substantiated by the findings that constitutive expression of Smad7 in HSCs completely abrogates transdifferentation to MFBs and reduces bile duct ligation (BDL)-dependent liver fibrosis in rats [20]. The role of TGF-β signaling in hepatocytes during chronic liver damage is yet not clear: Suppression of growth, structure and function of this cell type as well as induction of apoptosis is suggested, but molecular details are not thoroughly delineated [21]. Aim of the current study was to add *in vivo* data highlighting the previously reported predominant role of Smad3 - dependent TGF-β signaling in fibrogenesis. In a rat cholestasis model, fibrotic tissue is characterized by increased Smad3 signaling, as indicated by phosphoSmad3 analysis in total liver tissue lysates and nuclear Smad3 staining in hepatocytes surrounding fibrotic lesions. Unexpectedly, there is a progressive increase in intrahepatic Smad7 expression, which was mainly localized to HSCs.

Materials and methods

Materials

Taq polymerase and α-^{32}PdCTP were from Amersham/Pharmacia (Freiburg, Germany). Oligonucleotides were from MWG Biotech (Ebersberg, Germany).

Induction of fibrosis in rats

Male Sprague-Dawley rats (300 g body weight, Harlan-Winkelmann, Borchen, Germany) were kept temperature controlled (22°C) with a 12 h light/dark cycle and fed ad libitum with standard chow. Animals had free access to tap water. The common bile duct was located through a midline incision and double ligated near the liver hilus with transection between the ligatures [22]. Rats were anaesthetised with 100 mg/kg ketamine (Sanofi-ZEVA, Düsseldorf, Germany) and 6 animals were sacrificed on days 7, 14, 21, 28 and 35 post operation. Controls underwent a sham operation. All animals received care in compliance with the German Animal Protection Act, which is in accordance with the National Research Council's criteria. For Molecular Biology analysis, frozen livers were pulverized.

Quantitative Real-Time Reverse-Transcription PCR

1 μg RNA was reverse transcribed using Omniscript RT-PCR kit (Qiagen, Hilden, Germany). For quantitative

analysis of Smad7 mRNA, a LightCycler system from Roche (Mannheim, Germany) was used with the following primers (rat Smad7 forward: 5'-GGAGTCCTTTCCTCTCTC-3'; rat Smad7 reverse: 5'-GGCTCAATGAGCATGCTCAC-3'; MWG Biotech) and two fluorescence-dye labeled hybridization probes (5'-LC640AACCTGTTGTATTGCAGATTTGGG ACTTGCTG-Ph-3'; 5'AGCACTACGATGCTAAATTT CCGATGAG-fluorescin-3'; TIB Molbiol, Berlin, Germany). As a reference, cDNA corresponding to 200, 100, 50 or 25 ng total RNA of a mixture of all samples was tested. cDNAs of different samples were analysed, each corresponding to 100 ng reverse transcribed total RNA. Cycling reactions were performed as follows: 95 °C, 30 sec -1 cycle and 95°C, 1 sec; 60°C, 15 sec; 72°C, 10 sec -42 cycles. Subsequently, quantitative analysis of Smad4 and Smad7 mRNA was managed using hybridization dependent FRET signals (Smad7) or the QuantiTec SYBR Green PCR Kit (Qiagen, Smad4). Primer sequences for rat Smad4 were: rat Smad4 forward, 5'GATAGCGTCTGTGTGAACC-3'; rat Smad4 reverse, 5'-GTACTGGTGGCATTAGACTC3')

Hydroxyproline measurement

Frozen liver tissue was hydrolyzed in 2.0 ml 6 N HCl for 3 hrs at 130°C. The solution was neutralized to pH 7.0 with 2.5 N NaOH and diluted 40-fold with deionized H_2O. 2 ml diluted solution were mixed with 1.0 ml 0.05 M chloramine T solution and incubated for 20 minutes at room temperature. 1 ml 3.15 M perchloric acid was added and the solution was incubated for 5 minutes at room temperature. 1 ml 20% p-dimethylaminobenzaldehyde was added and the solution was incubated for 20 minutes at 60°C. Absorbance was determined at 557 nm, and hydroxyproline was calculated by comparison to a standard curve [23].

Isolation of total RNA, mRNA and Northern blot analysis

Tissue samples were homogenized in TRIZOL Reagent (GIBCO BRL, Eggenstein, Germany; 1 ml/100 mg tissue) using the UltraTurrax (IKA, Staufen, Germany). mRNA was isolated using the Oligotex mRNA Midi Kit (Qiagen; 0.04–0.05 mg mRNA per mg total RNA). For Northern blot analysis, one third of mRNA preparations from three different animals were pooled, electrophoresed in 1% agarose formaldehyde gels and transferred to GeneScreen nylon membranes (NEN DuPont, Boston, USA). After ultraviolet crosslinking, blots were hybridized as described [15]. A 610 bp Eco RI/Not I fragment was generated from plasmid pcDNA3.1-Flag-Smad7 [7], kindly provided by Peter ten Dijke. To detect GAPDH a 1.4-kb DNA probe containing rat GAPDH cDNA fragment was created from pBluGAP [24] by Eco RI digestion. The fragments were gel purified and labeled with ^{32}P-dCTP using a random primer labeling kit from Gibco BRL (Rockville, MD, USA).

Immunoblotting

Lysates from liver tissue were prepared with RIPA buffer (1 x TBS, 1 % Nonidet P-40, 0.5 % sodium deoxycholate, 0.1 % SDS); Protease Inhibitor Mix (Roche) and Phosphatase Inhibitor Mix (Sigma, München, Germany) were added. Lysates were cleaned and enriched with the Protein Clean Up and Enrichment Kit from Pierce (Bonn, Germany). 5 to 8 µg protein lysates from each of 6 animals representing one experimental group were pooled, separated by 8% SDS PAGE and transferred to 0.45 µm nitrocellulose membranes (Protran BA 85; Schleicher & Schüll, Germany). Nonspecific binding was blocked by 5% milk powder in TBST overnight at 4°C followed by incubation with primary antibodies (diluted at 1:2.000 in 2.5 % milk powder in TBST) overnight at 4°C. Blots were washed two times in TBS/0.05 % Tween20 (Bio-Rad, München, Germany) and three times in TBS for 5–10 min each. The secondary anti rabbit horseraddish peroxidase antibody (stock solution: 400 µg/ml; 1:50.000; Santa Cruz Biotechnology, CA, USA) was incubated for one hour at room temperature followed by five wash steps as described above. Bound antibodies were detected with Supersignal West Dura (Pierce) for 5 min and subsequent evaluated with a LumiImager (Roche). Antibodies used were murine monoclonal anti-α SMA (Roche); monoclonal anti Smad4, polyclonal antiSmad2 and Smad7 (Santa Cruz); anti Smad3 (Zytomed, Berlin, Germany); phospho-Smad2 and phospho-Smad3, kindly provided from P. ten Dijke, Leiden Univ Medical Center.

Immunohistochemistry

The liver was perfused under low pressure via the portal vein and thereafter excised, cut into small pieces,

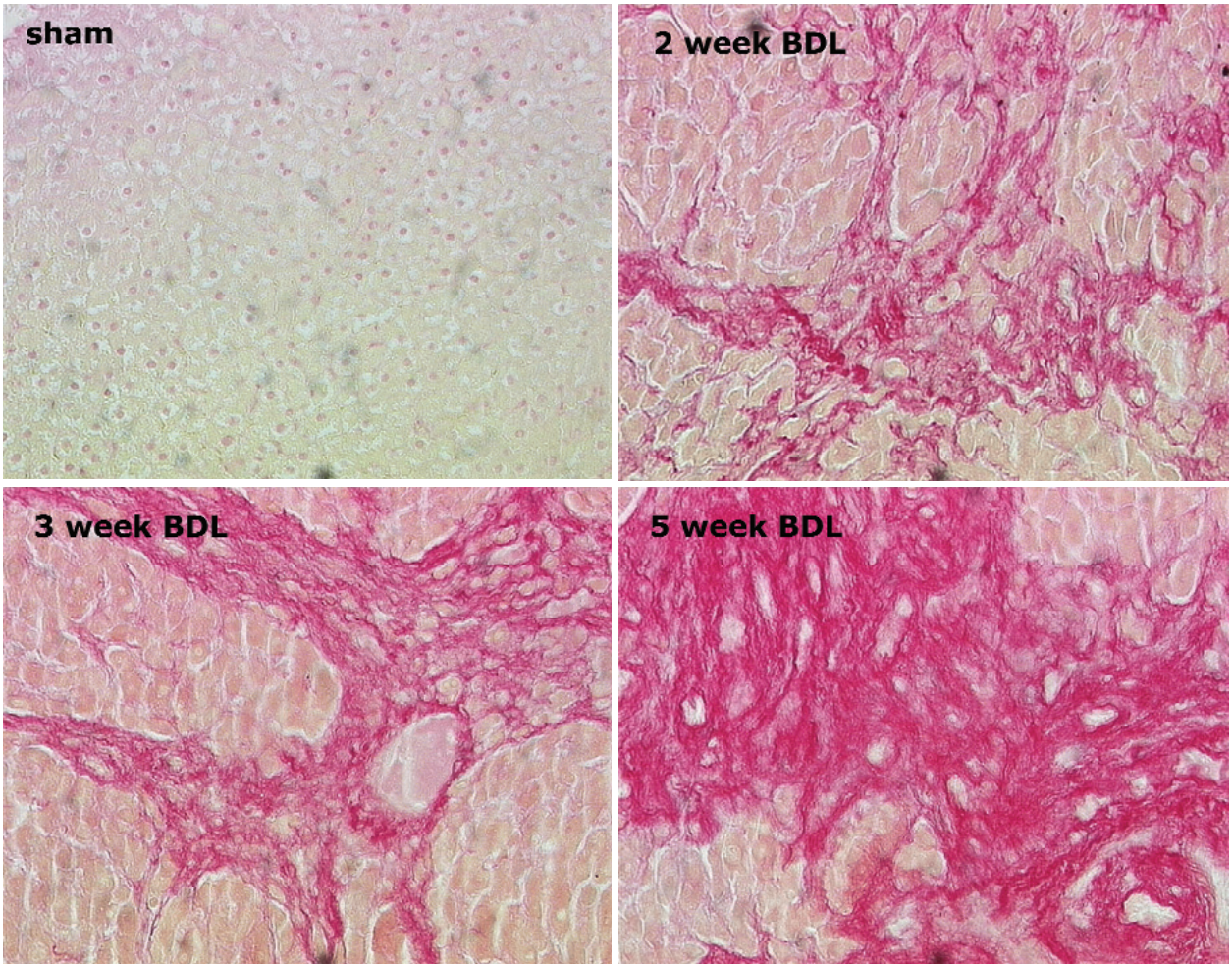

Fig. 1 Livers of rats with and without cholestasis due to bile duct ligation were resected and collagen deposition was examined by sirius red staining. Representative data for the indicated time points after BDL *vs.* sham operated animals are shown.

fixed in 4% paraformaldehyde in PBS, 10% formalin, and embedded in paraffin. 2 µm sections were deparaffinized and incubated for 30 min with hyaluronidase (1 mg/ml) in 100 mM Na-acetate, 150 mM NaCl, pH 5.5 for antigen demasking. Sections were then permeabilised on ice with 0.1% Triton X-100 in prechilled 0.1% Na-citrate buffer and in aceton (-20°C) for 90 sec. Antibodies used were monoclonal anti-α SMA (Roche), diluted 1:2.000. FITC labeled rabbit anti-mouse antibody (Santa Cruz) was used as secondary antibody at 1:200.

Picro sirius red staining was performed with 5 µm sections in staining solution (0.1g Sirius red, Polysciences, Eppelheim, Germany, in 100 ml picric acid) for 1h. Haematoxylin-Eosin and Ladewig stainings were performed according to standard procedures.

Results

Smad3 signaling is induced in bile duct ligation dependent fibrosis in rats

Histological evaluation of liver specimens from rats treated with BDL showed time-dependent increase in centrilobular and periportal ECM deposition. Fig. 1 displays representative liver samples from control and BDL animals taken at different time points after initiation of cholestasis and stained with picro sirius red to demonstrate collagen deposition. Correspondingly, hydroxyproline in total liver lysates was increased in BDL-rats (Fig. 2A). To further quantify the effects that BDL has on liver functions, serum concentrations of bilirubin and liver enzymes were determined (Fig. 2

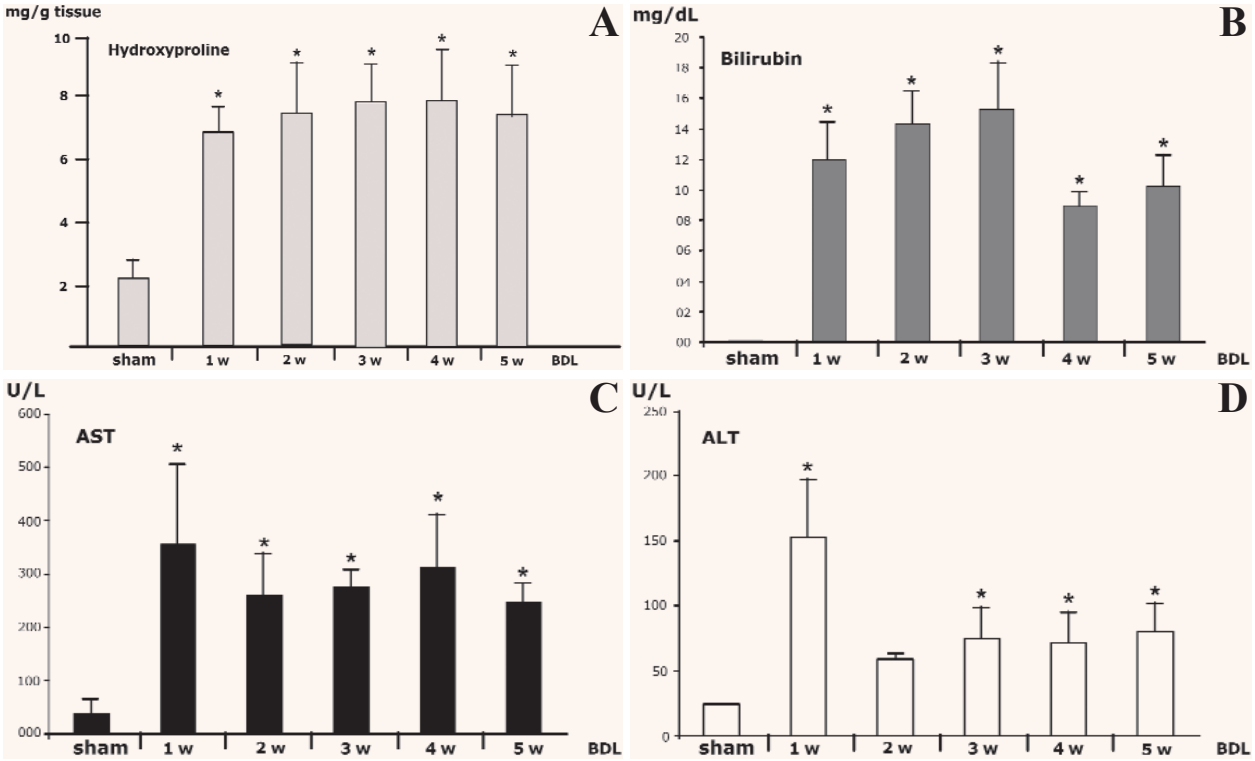

Fig. 2 (**A**) The hydroxyproline content in the liver of rats after bile duct ligation was measured at the indicated time points (n = 18; 3 samples from each of 6 rats; *P < 0.05 *vs.* sham operated animals on ranks and Student-Newman-Keuls test; w, weeks). Serum bilirubin (**B**), and serum values of hepatocyte transaminases, aspartate aminotransferase (AST, **C**) and alanine aminotransferase (ALT, **D**) in rats after bile duct ligation. Serum samples were collected at the indicated time points. Bilirubin, AST and ALT levels were determined by standard enzymatic methods. Mean values ± SEM in each group were plotted (n = 6, *P < 0.05 *vs.* sham operated animals on ranks and Student-Newman-Keuls test); w, week(s).

B–D). Within one week hydoxyproline levels were increased and remained within the same range for the whole experimental setting of 5 weeks. Similar rapid elevations and time courses were apparent for the other parameters, indicating progressive damage and upregulated collagen synthesis. Western blots from liver lysates and immunohistochemistry data from liver tissue sections demonstrate upregulated α-SMA expression with duration of cholestasis, indicating HSC proliferation and transdifferentiation (Fig. 3). Liver lysates from 6 animals treated for 2 and 4 weeks with BDL and from 4 sham operated controls were pooled and examined with phospho-Smad specific antibodies to test for activation of the TGF-β pathway (Fig. 4). Primary cultured HSCs from healthy rats at day 2 in culture were serum starved for 8 hrs and then treated for 1 h with 5 ng/ml TGF-β1. Corresponding lysates were used as positive control for Smad2/3 C-terminal phosphorylation. Our data display activation of TGF-β/Smad3 signaling in damaged tissue when compared to controls, whereas Smad2 phosphorylation was only slightly increased. Upregulated Smad3 phosphorylation was not accompanied by increased Smad3 expression.

Immunostainings with an antibody detecting selectively Smad3 show nuclear localization of Smad3 in nonparenchymal and virtually all parenchymal cells in fibrotic lesions of BDL damaged livers, whereas control animals were completely negative (Fig. 5).

Smad7 expression is continuously increased during bile duct ligation dependent fibrogenesis

Next, the expression of Smad4 and Smad7 mRNA in liver lysates was quantified. For Smad4, we used

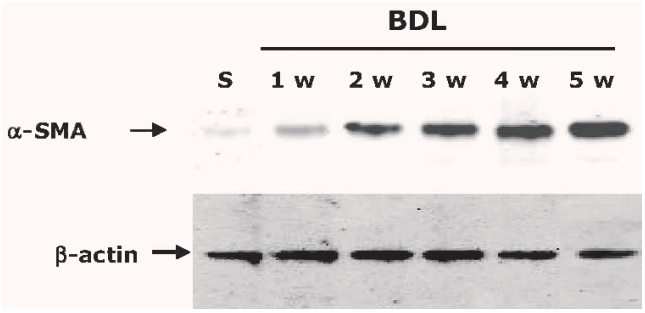

Fig. 3 A mixture of total liver protein lysates pooled from 6 animals (5 µg from each sample, 30 µg in total) was examined for α-SMA expression by Western blotting (upper part). The same blot was stripped and reprobed for β-actin antibody as a loading control; s, sham; w, week(s). In addition, liver sections were immunostained with a monoclonal anti-α-SMA antibody. A representative photomicrograph, showing positive α-SMA staining (brown color) in BDL treated rats *vs.* sham operated animals is shown (lower part).

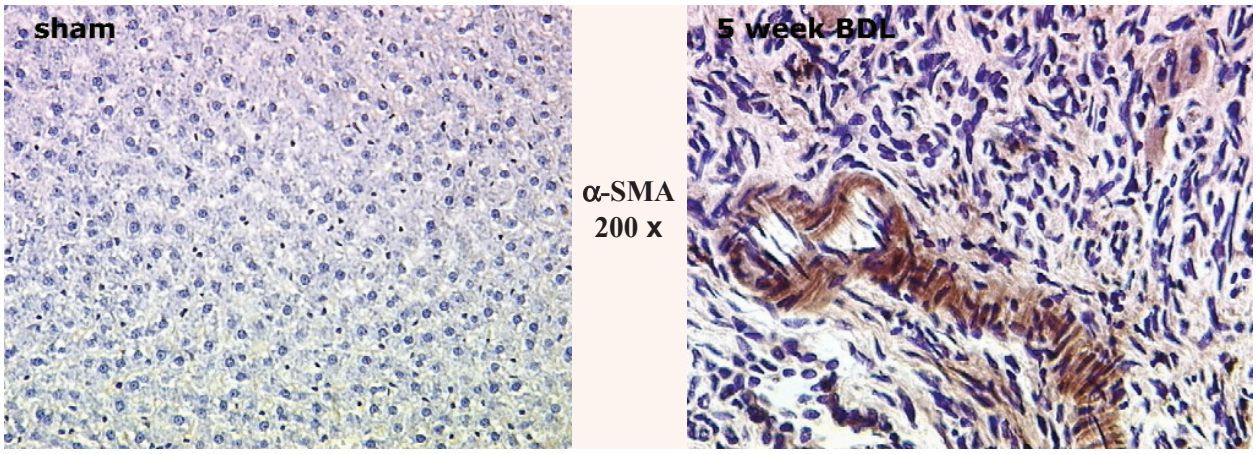

Cybergreen incorporation to measure real time amplification with rat Smad4 specific primers (Fig. 6 A). These data rather indicate a downregulation of Smad4 mRNA with cholestasis, at the same time no change of Smad4 protein levels was observed by Western blotting (Fig. 6 B). In contrast, Smad7 expression levels increased over time after BDL-induced cholestasis, as measured by RT-PCR with rat Smad7 specific primers (Fig. 7 A). The data were validated by Northern blotting with mRNA that was hybridized with a specific Smad7 cDNA probe (Fig. 7 B). Immunostainings of liver sections demonstrate that Smad7 is present in nonparenchymal cells, probably representing regulation of TGF-β signaling in activated proliferating HSCs (Fig. 5).

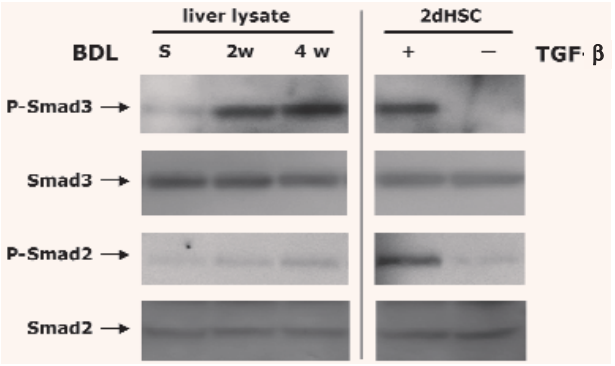

Fig. 4 Phosphorylation of Smad3 is induced in total liver lysates of rats treated with bile duct ligation. A mixture of total liver protein lysates pooled from 6 animals (8 µg from each sample, 48 µg in total) at each time point were analyzed by SDS-PAGE followed by Western blotting and immunodetection using specific antisera, as indicated. Quiescent (2 days) primary cultured rat hepatic stellate cells (HSCs), treated with 5 ng/ml TGF-β for 1 h were used as positive control for Smad phosphorylation. Parallel blots were probed in presence of blocking peptides, to which the antisera were originally raised, resulting in blank lanes (not shown), or with Smad2/3-specific antisera as indicated, to demonstrate relative Smad protein expression. Blots were reprobed with a monoclonal anti-b-actin antibody to confirm equal protein loading (not shown).

Discussion

As a consequence of chronic liver diseases deposition of ECM occurs with profound changes of the liver architecture [2]. Various cytokines are involved in disease pathogenesis. In particular, TGF-β1 is overexpressed in nonparenchymal cells of cirrhotic liver and plays a pivotal role in cirrho-

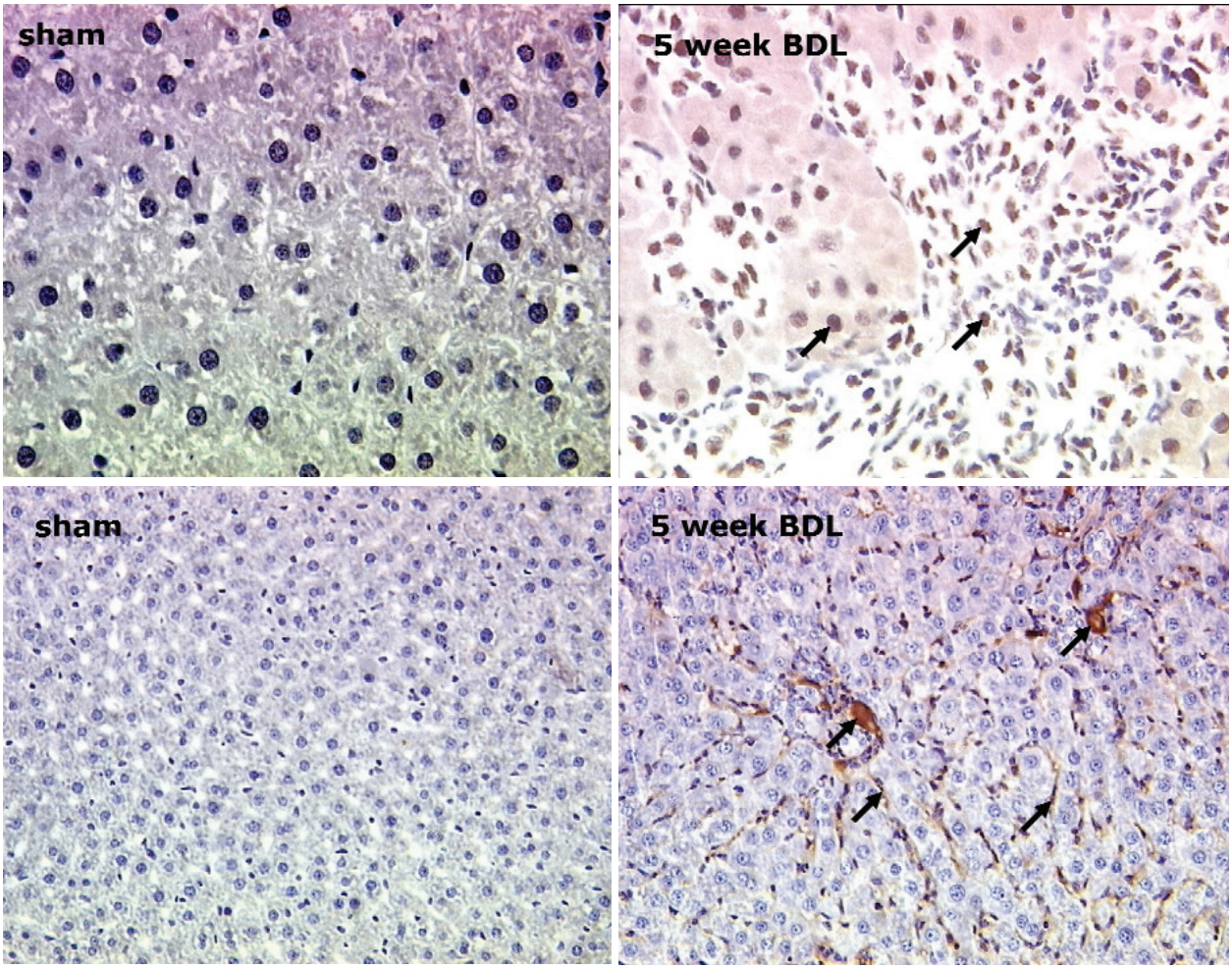

Fig. 5 Liver sections of sham operated or bile duct ligated rats were immunostained with polyclonal antisera against Smad3 and Smad7. Representative photomicrographs, showing positive nuclear Smad3 staining (brown color), mainly in hepatocytes from scar tissue of BDL-treated rats is visible. In contrast, positive Smad7 staining related to damaged liver tissue is mainly localized in regions between hepatocytes, probably representing activated but not fully tansdifferentiated HSCs.

sis development by stimulating activation of HSCs [4]. Furthermore, TGF-β inhibits hepatocyte proliferation and contributes to impaired hepatic regeneration. Therapeutic trials designed to inactivate TGF-β in liver cells blunted fibrogenesis, confirming the relevance of TGF-β signaling in chronic liver disease [20, 25–28]. We and others have investigated molecular details of TGF-β signaling in primary cultured

HSCs. Quiescent cells (2 days in culture) are sensitive to exogenous TGF-β and respond with Smad2/3 phosphorylation [14]. At this stage, Smad7 represents one of the target genes, initiating a negative feedback mechanism and leading to a fine tuning of TGF-β signaling [15]. Activated HSCs (7 days in culture) display a distinct TGF-β signalling response. These cells are stimulated autocrine by endogenously produced and secreted TGF-β and do not respond with Smad7 upregulation after exogenous addition of TGF-β1 [13]. These cells do not express Smad7 and overexpression of Smad7 by adenoviral infection completely abrogates the transdifferentiation process [20]. Similar findings were reported when comparing TGF-β signaling in acute and chronic rat liver injury [29]. Acute CCl_4 intoxication led to Smad2 phosphorylation and induction of Smad7 expression in HSCs, whereas chronic damage induced by CCl_4 treatment 3 times per week

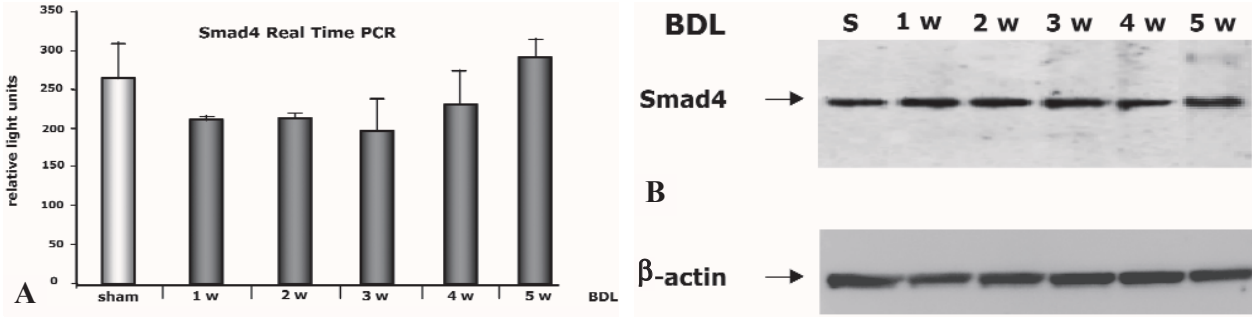

Fig. 6 Sybr-Green real time quantitative RT-PCR displayed a slightly downregulation of Smad4 mRNA expression in BDL treated rat liver recovering levels trending upward in proportion to the duration of chronic injury . Total RNA was purified from whole liver and 1 mg RNA was reverse transcribed to cDNA and real time quantitative RT-PCR was undertaken using the Light Cycler (Roche) with the QuantiTec SYBR Green PCR Kit(Qiagen, Hilden, Germany) according to the manufacturers protocol. As a standard reaction, cDNA corresponding to 200, 100, 50 or 25 ng total RNA of a mixture of all samples was exampled. Subsequently, cDNAs of different samples were analysed, each corresponding to 100 ng reverse transcribed total RNA. The results were interpreted according to the manufacturers instruction. Cycling steps were as follows 95°C, 15 minutes;1 cycle and 94°C, 15 sec;50°C, 20 sec; 72°C, 20 sec;45 cycles. The following two primer sequenzes rat Smad4 for 5´-GATAGCGTCTGTGTGAACC-3´; rat Smad4 rev 5´-GTACTGGTGGCATTAGACTC-3´ were used. The figure is representative for three independent experiments (mean values ± SD of n = 2).

for 3 and 6 weeks resulted in constitutive Smad2 phosphorylation and lack of Smad7 induction. The authors conclude that constitutive Smad2 phosphorylation by endogenous TGF-β under a low level of Smad7 could be involved in progression of liver fibrosis. This assumption is further supported by our data showing that overexpression of Smad7 under the CMV promoter in liver after adenoviral infection improves liver fibrogenesis in BDL rats. In the present study the Smad7 mRNA abundance increases with duration of BDL-induced cholestasis and liver fibrosis. Immunohistochemistry displays positive

Fig. 7 Sybr-Green real time quantitative RT-PCR displays increased mRNA expression of antagonistic Smad7 in BDL treated rat liver, levels trending upward in proportion to the duration of chronic injury. Total RNA was purified from whole liver and 1 mg RNA was reverse transcribed to cDNA and real time quantitative RT-PCR was undertaken using the Light Cycler (Roche) with the QuantiTec SYBR Green PCR Kit(Qiagen, Hilden, Germany) according to the manufacturers protocol. As a standard reaction, cDNA corresponding to 200, 100, 50 or 25 ng total RNA of a mixture of all samples was exampled. Subsequently, cDNAs of different samples were analysed, each corresponding to 100 ng reverse transcribed total RNA. The results were interpreted according to the manufacturers instruction. Cycling steps were as follows 95°C, 15 minutes;1 cycle and 94°C, 15 sec; 50°C, 20 sec; 72°C, 20 sec; 45 cycles. The following two amplification primers (rat Smad 7 for: 5`-GGAGTCCTTTCCTCTCTC-3`; rat Smad 7 rev: 5`GGCTCAATGAGCATGCTCAC-3`,MWG Biotech, Berlin, Germany) were used. The figure is representative for three independent experiments (mean values ± SD of n = 2).

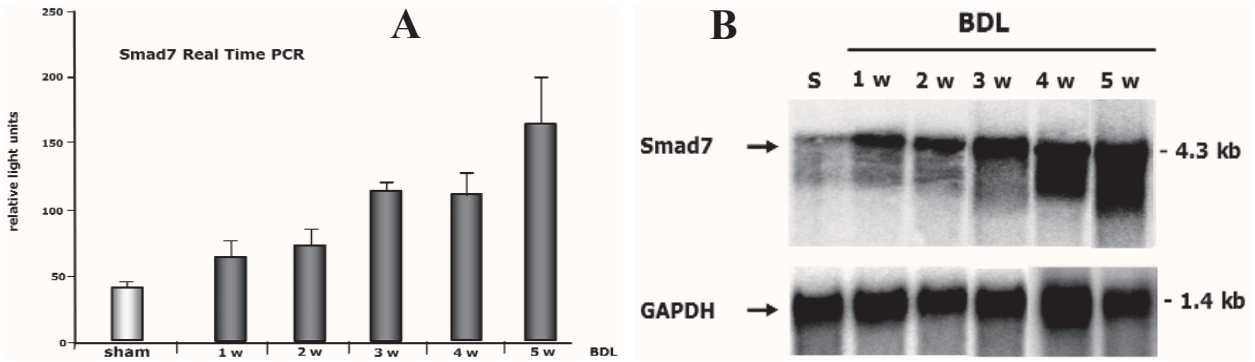

Smad7 staining in nonparenchymal cells of damaged regions which are also positive for α-SMA, most likely representing HSCs. According to the aforementioned model, the increased expression of Smad7 in HSCs of BDL rats might be explained by an increasing number of early activated HSCs that have a functional Smad7-dependent negative regulation of TGF-β signaling. On the other hand it cannot be excluded that *in vivo*, transdifferentiated MFBs are able to express Smad7 during fibrogenesis. Mice with a targeted deletion of Smad3 have demonstrated that profibrotic responses to TGF-β are mediated by Smad3 (for review see [30]). Smad3 null inflammatory cells and fibroblasts do not respond to the chemotactic effects of TGF-β and do not autoinduce TGF-β. The loss of Smad3 also interferes with TGF-β-mediated induction of endothelial to mesenchymal transition (EMT) and of genes for collagens, plasminogen activator inhibitor-1 and tissue inhibitor of metalloprotease-1. Smad3 null mice are resistant to radiation-induced cutaneous fibrosis, bleomycin-induced pulmonary-fibrosis, CCl_4-induced hepatic fibrosis as well as glomerular fibrosis induced by induction of type I diabetes with streptozotocin. In fibrotic conditions induced by EMT, such as proliferative vitreoretinopaty, ocular capsule injury and glomerulosclerosis resulting from unilateral ureteral obstruction, Smad3 null mice also show an abrogated fibrotic response. Animal models for scleroderma, cystic fibrosis and cirrhosis implicate involvement of Smad3 in the observed fibrosis. Additionally, inhibition of Smad3 by overexpression of Smad7 or by treatment with the small molecule halofuginone dramatically reduces responses in animal models of kidney, lung, liver and radiation-induced fibrosis. In HSCs, interaction of transcription factors Smad3 and SP1 mediate TGF-β-dependent stimulation of the Col1A2 promoter [31]. We and others have shown constitutively C-terminal phosphorylated Smad3 in CFSC2G, a cell line derived from HSCs purified from cirrhotic rat liver along with increased COL1A2 and PAI-1 gene expression and Smad binding element (SBE) activation in reporter gene analysis [18, 19]. Similar data were reported in primary cultured HSCs, which display predominant Smad2 signaling at day 2 in culture and a modulation of TGF-β signaling to the Smad3 pathway primarily in transdifferentiated MFBs [32]. In addition, increased phosphorylation of the linker region by the p38 MAPK pathway was described in primary cultures of HSCs and the authors propose that, as HSCs become fully differentiated to MFBs, the TGF-β RI-mediated Smad3 signal decreases and a p38 MAPK–mediated Smad3 signal predominates with the sequela of excess ECM synthesis and deposition [33]. Our data from BDL rats further support a prominent role of this pathway, since Smad3 and not Smad2 phosphorylation is enhanced after liver damage as assessed by Western blotting using whole liver lysates and phospho-Smad specific antisera. Interestingly, immunohistochemical data reveal that significant Smad3 signaling can be observed in hepatocytes from fibrotic lesions, indicating upregulated TGF-β signaling in hepatocytes during liver damage. It is hypothesized that TGF-β signaling in hepatocytes is directed to blunting liver regeneration by proliferation inhibition and/or apoptosis induction. In a recent study with Bcl-xL knock out mice, persistent apoptosis of hepatocytes was sufficient to induce fibrotic lesions in liver tissue and suggests a mechanistic link between apoptosis and fibrosis [34]. Further, generation of ECM producing interstitial fibroblasts from hepatocytes by EMT [34] and participation of TGF-β in such a process is conceivable.

In summary, the presented *in vivo* data regarding TGF-β signaling in chronic liver disease due to cholestasis further confirm a prominent role for Smad3, occurring predominantly in hepatocytes of fibrotic lesions. Unexpectedly, Smad7 expression is continuously increasing in nonparenchymal cells during cholestasis. These data indicate, that a functional negative regulation of TGF-β signaling in HSCs by Smad7 is not sufficient to blunt fibrogenesis *in vivo* and favor an important role of Smad3 activation in hepatocytes.

Acknowledgements

The study was funded by Sonderforschungsbereich 542 projects A4, C4 and C8; START fibrosis project of the University Hospital Aachen; the Dietmar Hopp Stiftung GmbH. E.W. was recipient of a Heinz-Breuer fellowship of the Deutsche Gesellschaft für Klinische Chemie und Laboratoriumsmedizin. We thank Sibylle Sauer-Lehnen and Bert Delvoux for excellent technical assistance.

References

1. **Geerts A.** History, heterogeneity, developmental biology, and functions of quiescent hepatic stellate cells. *Semin Liver Dis*. 2001; 21: 311–35.
2. **Friedman SL.** Liver fibrosis - from bench to bedside. *J Hepatol*. 2003; 38: S38–53.
3. **Kopp J, Seyhan H, Muller B, Lanczak J, Pausch E, Gressner AM, Dooley S, Horch RE.** N-acetyl-L-cysteine abrogates fibrogenic properties of fibroblasts isolated from Dupuytren's disease by blunting TGF-beta signalling. *J Cell Mol Med*. 2006; 10: 157–65.
4. **Gressner AM, Weiskirchen R, Breitkopf K, Dooley S.** Roles of TGF-beta in hepatic fibrosis. *Front Biosci*. 2002; 7: d793–807.
5. **ten Dijke P, Hill CS.** New insights into TGF -beta-Smad signalling. *Trends Biochem Sci*. 2004; 29: 265–73.
6. **Topper JN, Cai J, Qiu Y, Anderson KR, Xu YY, Deeds JD, Feeley R, Gimeno CJ, Woolf EA, Tayber O, Mays GG, Sampson BA, Schoen FJ, Gimbrone MA, Jr, Falb D.** Vascular MADs: two novel MAD-related genes selectively inducible by flow in human vascular endothelium. *Proc Natl Acad Sci USA*. 1997; 94: 9314–9.
7. **Nakao A, Afrakhte M, Moren A, Nakayama T, Christian JL, Heuchel R, Itoh S, Kawabata N, Heldin NE, Heldin CH, Tendijke P.** Identification of Smad7, a TGF beta-inducible antagonist of TGF -beta signalling. *Nature* 1997; 389: 631–5.
8. **Zhu HJ, Iaria J, Sizeland AM.** Smad7 differentially regulates transforming growth factor beta-mediated signaling pathways. *J Biol Chem*. 1999; 274: 32258–64.
9. **Afrakhte M, Moren A, Jossan S, Itoh S, Sampath K, Westermark B, Heldin CH, Heldin NE, ten Dijke P.** Induction of inhibitory Smad6 and Smad7 mRNA by TGF-beta family members. *Biochem Biophys Res Commun*. 1998; 249: 505–11.
10. **Bitzer M, von Gersdorff G, Liang D, Dominguez-Rosales A, Beg AA, Rojkind M, Bottinger EP.** A mechanism of suppression of TGF-beta/SMAD signaling by NF-kappa B/RelA. *Genes Dev*. 2000; 14: 187–97.
11. **Stopa M, Anhuf D, Terstegen L, Gatsios P, Gressner AM, Dooley S.** Participation of Smad2, Smad3, and Smad4 in transforming growth factor beta (TGF-beta)-induced activation of Smad7. THE TGF-beta response element of the promoter requires functional Smad binding element and E- box sequences for transcriptional regulation. *J Biol Chem*. 2000; 275: 29308–17.
12. **Ulloa L, Doody J, Massague J.** Inhibition of transforming growth factor-beta/SMAD signalling by the interferon-gamma/STAT pathway. *Nature* 1999; 397: 710–3.
13. **Dooley S, Delvoux B, Lahme B, Mangasser-Stephan K, Gressner AM.** Modulation of transforming growth factor beta response and signaling during transdifferentiation of rat hepatic stellate cells to myofibroblasts. *Hepatology* 2000; 31: 1094–106.
14. **Dooley S, Delvoux B, Streckert M, Bonzel L, Stopa M, ten Dijke P, Gressner AM.** Transforming growth factor beta signal transduction in hepatic stellate cells via Smad2/3 phosphorylation, a pathway that is abrogated during *in vitro* progression to myofibroblasts. TGFbeta signal transduction during transdifferentiation of hepatic stellate cells. *FEBS Lett*. 2001; 502: 4–10.
15. **Dooley S, Streckert M, Delvoux B, Gressner AM.** Expression of Smads during *in vitro* transdifferentiation of hepatic stellate cells to myofibroblasts. *Biochem Biophys Res Commun*. 2001; 283: 554–62.
16. **Gressner AM, Weiskirchen R.** Modern pathogenetic concepts of liver fibrosis suggest stellate cells and TGF-beta as major players and therapeutic targets. *J Cell Mol Med*. 2006; 10: 76–99.
17. **Breitkopf K, Lahme B, Tag CG, Gressner AM.** Expression and matrix deposition of latent transforming growth factor beta binding proteins in normal and fibrotic rat liver and transdifferentiating hepatic stellate cells in culture. *Hepatology* 2001; 33: 387–96.
18. **Berg F, Delvoux B, Gao C, Westhoff JH, Breitkopf K, Gressner AM.** Divergence of TGF-β signaling in activated hepatic stellate cells downstream from Smad2 phosphorylation. *Signal Transduction* 2002; 1–3: 1–18.
19. **Inagaki Y, Mamura M, Kanamaru Y, Greenwel P, Nemoto T, Takehara K, Ten Dijke P, Nakao A.** Constitutive phosphorylation and nuclear localization of Smad3 are correlated with increased collagen gene transcription in activated hepatic stellate cells. *J Cell Physiol*. 2001; 187: 117–23.
20. **Dooley S, Hamzavi J, Breitkopf K, Wiercinska E, Said HM, Lorenzen J, Ten Dijke P, Gressner AM.** Smad7 prevents activation of hepatic stellate cells and liver fibrosis in rats. *Gastroenterology* 2003; 125: 178–91.
21. **Horch RE.** Future perspectives in tissue engineering. *J Cell Mol Med*. 2006; 10: 4–6.
22. **Kountouras J, Billing BH, Scheuer PJ.** Prolonged bile duct obstruction: A new experimental model for cirrhosis in the rat. *Br J Exp Path.* 1984; 65: 305–11.
23. **Jamall IS, Finelli VN, Que Hee SS.** A simple method to determine nanogram levels of 4hydroxyproline in biological tissues. *Anal Biochem*. 1981; 112: 70–5.
24. **Tokunaga K, Nakamura Y, Sakata K, Fujimori K, Ohkubo M, Sawada K, Sakiyama S.** Enhanced expression of a glyceraldehyde-3-phosphate dehydrogenase gene in human lung cancers. *Cancer Res*. 1987; 47: 5616–9.
25. **George J, Roulot D, Koteliansky VE, Bissell DM.** *In vivo* inhibition of rat stellate cell activation by soluble transforming growth factor beta type II receptor: A potential new therapy for hepatic fibrosis. *Proc Nat Acad Sci USA*. 1999; 96: 12719–24.
26. **Qi Z, Atsuchi N, Ooshima A, Takeshita A, Ueno H.** Blockade of type beta transforming growth factor signaling prevents liver fibrosis and dysfunction in the rat. *Proc Nat Acad Sci USA*. 1999; 96: 2345–9.

27. **Yata Y, Gotwals P, Koteliansky V, Rockey DC.** Dose-dependent inhibition of hepatic fibrosis in mice by a TGF-beta soluble receptor: implications for antifibrotic therapy. *Hepatology* 2002; 35: 1022–30.
28. **Okuno M, Akita K, Moriwaki H, Kawada N, Ikeda K, Kaneda K, Suzuki Y, Kojima S.** Prevention of rat hepatic fibrosis by the protease inhibitor, camostat mesilate, via reduced generation of active TGF-beta. *Gastroenterology* 2001; 120: 1784–800.
29. **Tahashi Y, Matsuzaki K, Date M, Yoshida K, Furukawa F, Sugano Y, Matsushita M, Himeno Y, Inagaki Y, Inoue K.** Differential regulation of TGF-beta signal in hepatic stellate cells between acute and chronic rat liver injury. *Hepatology* 2002; 35: 49–61.
30. **Flanders KC.** Smad3 as a mediator of the fibrotic response. *Int J Exp Pathol*. 2004; 85: 47–64.
31. **Inagaki Y, Nemoto T, Nakao A, Dijke P, Kobayashi K, Takehara K, Greenwel P.** Interaction between GC box binding factors and Smad proteins modulates cell lineage-specific alpha 2(I) collagen gene transcription. *J Biol Chem*. 2001; 276: 16573–9.
32. **Liu C, Gaca MD, Swenson ES, Vellucci VF, Reiss M, Wells RG.** Smads 2 and 3 are differentially activated by transforming growth factor-beta (TGF-beta) in quiescent and activated hepatic stellate cells. Constitutive nuclear localization of Smads in activated cells is TGF-betaindependent. *J Biol Chem*. 2003; 278: 11721–8.
33. **Furukawa F, Matsuzaki K, Mori S, Tahashi Y, Yoshida K, Sugano Y, Yamagata H, Matsushita M, Seki T, Inagaki Y, Nishizawa M, Fujisawa J, Inoue K.** p38 MAPK mediates fibrogenic signal through Smad3 phosphorylation in rat myofibroblasts. *Hepatology* 2003; 38: 879–89.
34. **Takehara T, Tatsumi T, Suzuki T, Rucker EB, 3rd, Hennighausen L, Jinushi M, Miyagi T, Kanazawa Y, Hayashi N.** Hepatocyte-specific disruption of Bcl-xL leads to continuous hepatocyte apoptosis and liver fibrotic responses. *Gastroenterology* 2004; 127: 1189–97.